Wnt7b stimulates embryonic lung growth by coordinately increasing the replication of epithelium and mesenchyme

Jayaraj Rajagopal[1,2,3], Thomas J. Carroll[4], J. Sawalla Guseh[1,2,3], Sam A. Bores[1,2], Leah J. Blank[1,2], William J. Anderson[1,2], Jing Yu[5], Qiao Zhou[1,2], Andrew P. McMahon[1] and Douglas A. Melton[1,2,*]

The effects of Wnt7b on lung development were examined using a conditional *Wnt7b*-null mouse. *Wnt7b*-null lungs are markedly hypoplastic, yet display largely normal patterning and cell differentiation. In contrast to findings in prior hypomorphic *Wnt7b* models, we find decreased replication of both developing epithelium and mesenchyme, without abnormalities of vascular smooth muscle development. We further demonstrate that Wnt7b signals to neighboring cells to activate both autocrine and paracrine canonical Wnt signaling cascades. In contrast to results from hypomorphic models, we show that Wnt7b modulates several important signaling pathways in the lung. Together, these cascades result in the coordinated proliferation of adjacent epithelial and mesenchymal cells to stimulate organ growth with few alterations in differentiation and patterning.

KEY WORDS: Lung organogenesis, Wnt signaling, Organ growth

INTRODUCTION

Wnt proteins play important roles in the growth and morphogenesis of many organs. In lung, Wnt signaling has been proposed to stimulate the proliferation of undifferentiated progenitors (De Langhe et al., 2005; Mucenski et al., 2003; Okubo and Hogan, 2004; Okubo et al., 2005), to affect proximodistal patterning (Mucenski et al., 2003; Shu et al., 2005), and to regulate branching morphogenesis (Dean et al., 2005). Multiple Wnt ligands, Frizzled receptors, and endogenous inhibitors of Wnt activity including Dkk, Sfrp and Kremen proteins add to the complexity of Wnt signaling in the lung (De Langhe et al., 2005; Shu et al., 2002). As a result, no simple consensus model of Wnt action has emerged (Cardoso and Lu, 2006).

Experiments altering Wnt signaling in the lung have yielded conclusions that are difficult to reconcile. The use of Wnt ligands (Dean et al., 2005) or Wnt antagonists (De Langhe et al., 2005) in culture is likely to promiscuously modify multiple Wnt interactions, and these considerations might explain, in part, why a Wnt antagonist produces a decrease in epithelial branching (De Langhe et al., 2005), whereas the morpholino knockdown of β-catenin results in enhanced branching (Dean et al., 2005). Additionally, phenotypes in lung patterning following epithelial β-catenin deletion (Mucenski et al., 2003; Shu et al., 2005) could be a result of altered Wnt signaling or of non-signaling effects of β-catenin elimination (Dean et al., 2005). We therefore used in vivo genetic deletion of a single Wnt ligand to clarify its effect on lung development.

The distal lung bud tip is the site of greatest cell proliferation in the embryonic lung (Cardoso and Lu, 2006; Eblaghie et al., 2006; Liu and Hogan, 2002; Okubo et al., 2005; Perl et al., 2002; Rawlins and Hogan, 2006; Warburton et al., 2000). Wnt5a and Wnt7b are both expressed most highly in this location (Shu et al., 2002; Wang

et al., 2005; Weidenfeld et al., 2002). *Wnt5a*-null mice exhibit increased cell proliferation in both epithelium and mesenchyme with a resulting expansion of the distal lung and increased lung size (Li et al., 2002). In this study, we focused on the action of Wnt7b.

A null mutation of *Wnt7b* deleting most of exon 3 and exon 4 (*Wnt7b*D3-4, see Fig. S1 in the supplementary material) results in early placental lethality (Parr et al., 2001), precluding an analysis of its role in lung growth. A second allele, *Wnt7b*lacZ, was created in which exon 1 (including the endogenous initiation codon and the predicted signal sequence) was replaced with *lacZ* and a *PGK-Neomycin* cassette (see Fig. S1 in the supplementary material). Homozygous *Wnt7b*lacZ animals bypass placental lethality and are born with hypoplastic lungs (Shu et al., 2002). We generated a third allele, *Wnt7b*D1, in which exon 1 (including the ATG codon and the predicted signal sequence) was deleted (see Fig. S1 in the supplementary material) (Lobov et al., 2005). Surprisingly, *Wnt7b*D1 homozygotes with a genetic deletion analogous to that of the *Wnt7b*lacZ homozygotes are viable and fertile, without a respiratory defect. The *Wnt7b*D1 allele is obviously hypomorphic, but displays decreased in vivo Wnt-reporter activity and phenotypes associated with loss of Wnt activity (Lobov et al., 2005). We now show that the *Wnt7b*D1 allele is hypomorphic due to alternative exon 1 splicing. Alternative splicing is also predicted to occur in the *Wnt7b*lacZ allele. To generate an unambiguous conditional null allele, we created another mutant allele designated *Wnt7b*C3 (see Fig. 1A), which conditionally deletes exon 3 when Cre recombinase is present to produce the *Wnt7b*D3-null allele (Fig. 1A and see Fig. S1 in the supplementary material).

We show that *Wnt7b*D3 homozygotes have markedly hypoplastic lungs. In contrast to the *Wnt7b*lacZ hypomorphic lungs, the lungs of *Wnt7b*D3 homozygotes display similarly decreased proliferation in both mesenchyme and epithelium throughout embryonic development. Furthermore, they possess incomplete tracheal cartilaginous rings and minor branching defects not noted in the prior hypomorphic animals. Interestingly, *Wnt7b*D3 homozygous lungs manifest largely normal cell-fate specification and tissue geometry including, and in contrast to the *Wnt7b*lacZ mice, normal vascular smooth muscle development. This genuine null model now reveals that Wnt7b does interact with known important lung mitogenic pathways. We further

[1]Department of Molecular and Cellular Biology, Harvard Stem Cell Institute, Harvard University, Cambridge, MA 02138, USA. [2]Howard Hughes Medical Institute, [3]Department of Internal Medicine, Massachusetts General Hospital, Boston, MA 02114, USA. [4]Department of Internal Medicine, Department of Molecular Biology, University of Texas Southwestern Medical Center, Dallas, TX 75390, USA. [5]Department of Cell Biology, University of Virginia, Charlottesville, VA 22908, USA.

*Author for correspondence (e-mail: dmelton@harvard.edu)

demonstrate that Wnt7b activates an autocrine epithelial and a paracrine mesenchymal canonical Wnt signaling mechanism. Together, these cascades stimulate the replication of both epithelium and mesenchyme in concert. The preservation of most aspects of cell fate differentiation and lung architecture, in the setting of profoundly decreased growth, suggest a surprising specificity in the action of Wnt7b.

MATERIALS AND METHODS
Mice
Male mice doubly heterozygous for the *Sox2-Cre* transgene (Hayashi et al., 2002) and the null *Wnt7b*[D3] allele were crossed with female mice that were homozygous for the floxed conditional allele of *Wnt7b*[C3]. This conditional allele produces the *Wnt7b*[D3]-null allele after Cre-mediated excision of exon 3. The details of the targeting for this allele and *Wnt7b*[D1] are available upon request and the complete results of an allelic series of *Wnt7b* mutants (T.J.C. and A.P.M., unpublished) will be presented elsewhere. All *Wnt7b* mutant lines were maintained on an identical (129/SvJ × SW) background. Progeny of the above cross were genotyped using the following primers: *Sox2Cre* Fwd, 5′-CTCTAGAGCCTCTG-CTAACC-3′ and *Sox2Cre* Rev, 5′-CCTGGCGATCCCTGAACATG-TCC-3′ (400 bp); *Wnt7b* null (Parr) Fwd, 5′-GGGGAATTCCGGG-CGTGGCGCATGCTGTC-3′ and *Wnt7b* null (Parr) Rev, 5′-GCAGG-CATGCTGGGGATGCGG-3′ (300 bp); *Wnt7b* conditional allele Fwd, 5′-TGACAGAGGATGGGGAGAAG-3′ and *Wnt7b* conditional allele Rev, 5′-GGTCTTTCCAAGGGTGGTCT-3′ (200 bp); *Wnt7b* exon 3 Cre-excised null allele Fwd, 5′-GAGGAAGTCAGGCAGGTGTC-3′ and *Wnt7b* exon 3 Cre-excised null allele Rev, 5′-TATCCCACCGAT-ACGCAAAC-3′(354 bp).

Tissue preparation
Lungs for immunohistochemistry were fixed in 4% paraformaldehyde for 1 hour at 4°C, and embedded in OCT or paraffin. For in situ hybridization (ISH), lungs were fixed overnight at 4°C. For whole-mount ISH, the lungs were dehydrated in methanol. For section ISH, lungs were dehydrated and embedded in paraffin.

In situ hybridization
Section and whole-mount ISH with digoxigenin-labeled probes was performed as previously described (Gray et al., 2004). The plasmid used to generate the *Bmp4* probe was a gift from B. Hogan (Duke University, Durham, NC). Plasmids for *Fgf10* and *Lef1* probes were gifts from S. Bellusci (University of Southern California, Los Angeles, CA). Remaining probes were obtained from a genome-wide transcription factor library (Gray et al., 2004).

BrdU incorporation and detection
Pregnant mice received intraperitoneal injection of BrdU (Amersham Bioscience, UK) as recommended by the manufacturer. After 1 hour, lungs were harvested and fixed. The paired *t*-test was used to assay for proliferation and $P<0.05$ was considered significant.

TUNEL
Apoptosis was assayed using the Dead End Apoptosis Detection System (Promega).

Immunohistochemistry
Primary antibodies used were: rabbit anti-CC10 1:50 (Santa Cruz); rat anti-E-cadherin 1:2000 (Zymed); rabbit anti-fibronectin 1:100 (Chemicon); rabbit anti-N-myc 1:100 (Santa Cruz); rat anti-PECAM 1:100 (BD Pharmingen); mIgG$_{2a}$ anti-smooth muscle actin 1:200 (Sigma); rabbit anti-smooth muscle myosin 1:100 (Biomedical Technologies); goat anti-Sox2 1:50 (Santa Cruz); goat anti-Sox9 1:50 (Santa Cruz); rabbit anti-pro-surfactant protein C (SP-C) 1:200 (Upstate); mIgG$_{2a}$ anti-BrdU 1:100 (Amersham Biosciences).

Secondary antibodies were conjugated to Alexa-Fluor 568 (1:500, Invitrogen). Slides prepared for BrdU detection were treated with citrate buffer (1.8 mM citric acid, 8.2 mM sodium citrate, pH 6.0) for 10 minutes at 89°C. Slides prepared for N-myc detection were treated with 1 mM EDTA for 10 minutes at 89°C.

Cell counting
Representative images from multiple tissue samples were counted. Approximately 7500 cells were counted in the tracheal epithelium and the distal airway. For Sox9-positive cells, 868 and 869 cells were counted in mutant and wild-type lungs, respectively. For cells in the alveolar sacs, 7532 cells, evenly divided between mutant and wild-type samples, were counted. When evaluating BrdU incorporation, a total of 13,304 cells were counted. Endoderm cells surrounded by smooth muscle were counted as stalk cells, whereas more distal endoderm cells were counted as tip cells.

Explant culture
Whole lung, isolated mesenchyme (Weaver et al., 2003), and recombined endoderm and mesenchyme culture (Bellusci et al., 1997a; Weaver et al., 2000) were performed. Whole lungs were dissected at E12.5 in PBS and grown in 50% DMEM (Gibco), 50% Ham's F12 (CellGrow), with penicillin, streptomycin, and glutamine (Gibco) at 37°C for 24 to 48 hours on Nucleopore Track-Etch membrane filters (Whatman). Dkk1 at 200 ng/ml (R&D Systems), LiCl at 20 mM, and Bmp4 at 100 ng/ml (R&D Systems) were added to the media as described.

RESULTS
Wnt7b consists of two different isoforms generated by alternative exon 1 usage
Previously reported *Wnt7b* alleles were designed to result in a null phenotype by removing exon 1 along with its start codon and predicted signal sequence (see Fig. S1 in the supplementary material) (Lobov et al., 2005; Shu et al., 2002). However, neither of these alleles phenocopied the early lethality associated with the *Wnt7b*[D3-4] allele, even though *Wnt7b*[D1] homozygotes were on an identical background. Either the removal of exon 1 resulted in a partial loss-of-function allele, or the more severe *Wnt7b*[D3-4] allele acted as a dominant-negative. The presence of transcripts containing the third exon in *Wnt7b*[lacZ] mice is consistent with the former possibility (Shu et al., 2002), and the hypothesis that the more severe *Wnt7b*[D3-4] allele acts as a dominant-negative allele is unlikely because heterozygous animals display no phenotype (Parr et al., 2001).

Previous studies have shown that some Wnts exist as distinct protein isoforms. To test the possibility that the *Wnt7b*[D1] animals are incomplete nulls due to the existence of an alternative exon 1, we performed RNase protection assays with a probe spanning exon 2 and the previously identified exon 1. This analysis suggested that there are indeed two isoforms of Wnt7b (see Fig. S2 in the supplementary material). Subsequent 5′ RACE identified an alternative *Wnt7b* transcript that utilizes a distinct first exon with its own ATG and a highly conserved signal sequence (see Fig. S2 in the supplementary material). We identified corresponding transcripts in the NCBI nucleotide database and E14.5 lung (see Fig. S2 in the supplementary material). In *Wnt7b*[D1] homozygous animals, we saw upregulation of the alternative transcript (see Fig. S2 in the supplementary material). These transcripts are likely to correspond to the residual exon 3 transcripts that were present in the *Wnt7b*[lacZ] hypomorphic mutants, strongly suggesting that alternative splicing occurs in *Wnt7b*[lacZ] homozygotes (Shu et al., 2002). Thus, *Wnt7b*[D3-4] mice represent a true null phenotype, whereas the other two alleles represent a partial loss-of-function.

Generation of a conditional null allele of *Wnt7b*
To characterize the role of Wnt7b in the lung, we used a conditional strategy to remove Wnt7b function from the entire embryo but not the placenta. The conditional knock-in allele, *Wnt7b*[C3], contains loxP sites flanking exon 3, and generates the null allele *Wnt7b*[D3] upon Cre-mediated removal of exon 3. *Wnt7b*[D3] was designed to mimic the true

null $Wnt7b^{D3-4}$ allele (see Fig. S1 in the supplementary material). Furthermore, $Wnt7b^{D3}$ does not retain a constitutively active promoter driving a neomycin resistance cassette, which has resulted in neomorphic effects in other systems (see Fig. S1 in the supplementary material). Germline removal of $Wnt7b^{D3}$ results in placental lethality as expected, similar to that of the original $Wnt7b^{D3-4}$ mutants. We next used a *Sox2-Cre* transgenic driver line (Hayashi et al., 2002), in which Cre is produced only in the epiblast, to recombine $Wnt7b^{C3}$ throughout the embryo proper, well before organogenesis. Conversely, extraembryonic tissues, including placenta, where *Sox2-Cre* is not expressed, retain the phenotypically wild-type $Wnt7b^{C3}$ conditional allele. Using this strategy, phenotypically normal $Wnt7b^{C3}$ homozygous mice were mated with the phenotypically normal doubly heterozygous *Sox2-Cre; $Wnt7b^+Wnt7b^{D3}$* mice (Fig. 1A). We expected 25% of pups to possess two null $Wnt7b^{D3}$ alleles (Fig. 1A). When present, *Sox2-Cre* expression completely converted the $Wnt7b^{C3}$ allele to $Wnt7b^{D3}$ in all E9.5 embryonic tissues (see Fig. S3 in the supplementary material).

Severe lung hypoplasia in $Wnt7b^{D3}$-null mice

Homozygous $Wnt7b^{D3}$ (hereafter referred to as *Wnt7b*-null) pups were born at the expected Mendelian ratio but became cyanotic despite chest wall movements and died within hours. These animals possessed markedly hypoplastic lungs and no expression of Wnt7b could be detected by ISH or RT-PCR (see Fig. S3 in the supplementary material). The lungs displayed less severe hemorrhage around major blood vessels when compared with $Wnt7b^{lacZ}$ hypomorphic lungs, and also manifested frequent alveolar hemorrhage not noted in $Wnt7b^{lacZ}$ mice (see Fig. S4 in the supplementary material) (Shu et al., 2002). Air was present throughout the trachea and bronchi but the lung was poorly inflated. Pups that possessed at least one functional *Wnt7b* allele ($n=31$) were phenotypically normal. At E18.5, mutant lungs weighed less than 50% of littermate controls ($P=0.0002$) (Fig. 1B). At E14.5, mutant lungs weighed less than 25% of littermate controls ($P<0.0001$) (Fig. 1C), and lungs from control animals comprised 2.25% of body mass, whereas those of *Wnt7b* lungs comprised only 0.22% of embryonic mass ($P<0.0001$). No general developmental delay was observed and the weight of the heart ($P=0.986$), liver ($P=0.6498$) and of the whole embryo ($P=0.3561$) were similar to control littermates at E14.5 and E18.5. As the diaphragm, liver, abdominal cavity and cardiac chambers appeared normal, the primary defect was likely to be in lung development.

At E12.5, mutant lungs were visibly smaller (Fig. 1D), but their lobar branching was largely preserved. The correct number of lobes was formed, but the medial lobe bronchus of the right lung emanated from the cephalic lobe bronchus in the *Wnt7b* mutant (Fig. 1D). At E14.5, mutant lungs had fewer distal tips and displayed a relative thinning of the mesenchyme (Fig. 2A-D and see Fig. S3 in the supplementary material). A wild-type E14.5 lung has ~1000 distal tips abutting the mesothelium, whereas the mutant lung had ~500 tips. The trachea appeared normal in diameter and length with an intact epithelium and normal smooth muscle. However, in contrast to $Wnt7b^{lacZ}$ mice, the cartilaginous rings of the trachea were incomplete (data not shown).

Normal cell differentiation and patterning are preserved in *Wnt7b*-null lungs

We next examined cell fate differentiation both qualitatively and quantitatively. At E14.5, normally distributed networks of PECAM (Pecam1)-positive endothelial cells are present in the proximal and distal lung (Fig. 2A). Smooth muscle surrounds the proximal
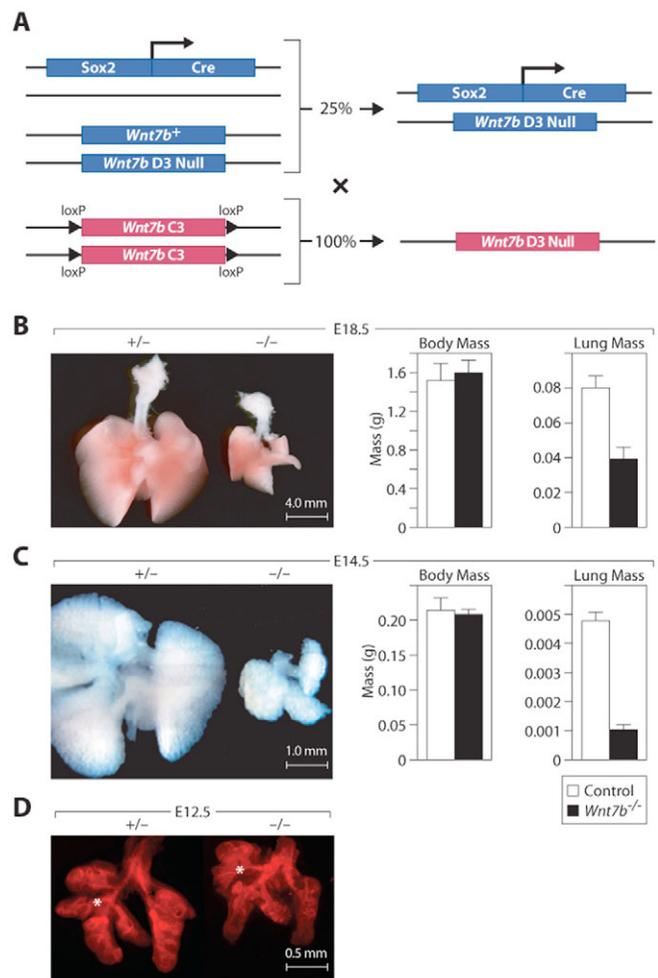

Fig. 1. Deletion of mouse *Wnt7b* results in hypoplastic lungs. (**A**) Strategy to remove *Wnt7b* from only the embryo proper. (**B**) Mutant lungs are 50% smaller than wild-type at E18.5. The overall mass of the embryo is unchanged. (**C**) Mutant lungs are 75% smaller than wild-type at E14.5. The overall mass of the embryo is unchanged. (**D**) Control and mutant lungs at E12.5. E-cadherin staining shows grossly normal lobulation in mutant lungs. However, the right medial lobe bronchus (*) of the *Wnt7b* mutant lung emanates from the cephalic lobe bronchus.

airways and vasculature and was appropriately absent around distal tip endoderm (Fig. 2B). The proximal airway marker Sox2 was expressed appropriately in the trachea and proximal airways and was excluded from distal endoderm (Fig. 2C), whereas Sox9 was appropriately expressed in the distal tip endoderm and excluded proximally (Fig. 2D).

Normal differentiation and patterning were also seen at E18.5 (Fig. 2E-H). Blood vessels adopted characteristic vascular networks (Fig. 2E) and smooth muscle surrounded proximal airways and blood vessels (Fig. 2F). We found no evidence of vascular smooth muscle abnormality, including previously described hypertrophy or apoptosis (see Fig. S4 in the supplementary material) (Shu et al., 2002). CC10 (Scgb1a1 – Mouse Genome Informatics), a proximal epithelial marker, was present in the airways and was appropriately absent distal to the bronchoalveolar duct junction (Fig. 2G). Finally, type 2 cells expressing SP-C (Sftpc – Mouse Genome Informatics) occurred in the distal saccules (Fig. 2H), whereas type 1 cells were present in decreased numbers in the alveoli (Fig. 2I).
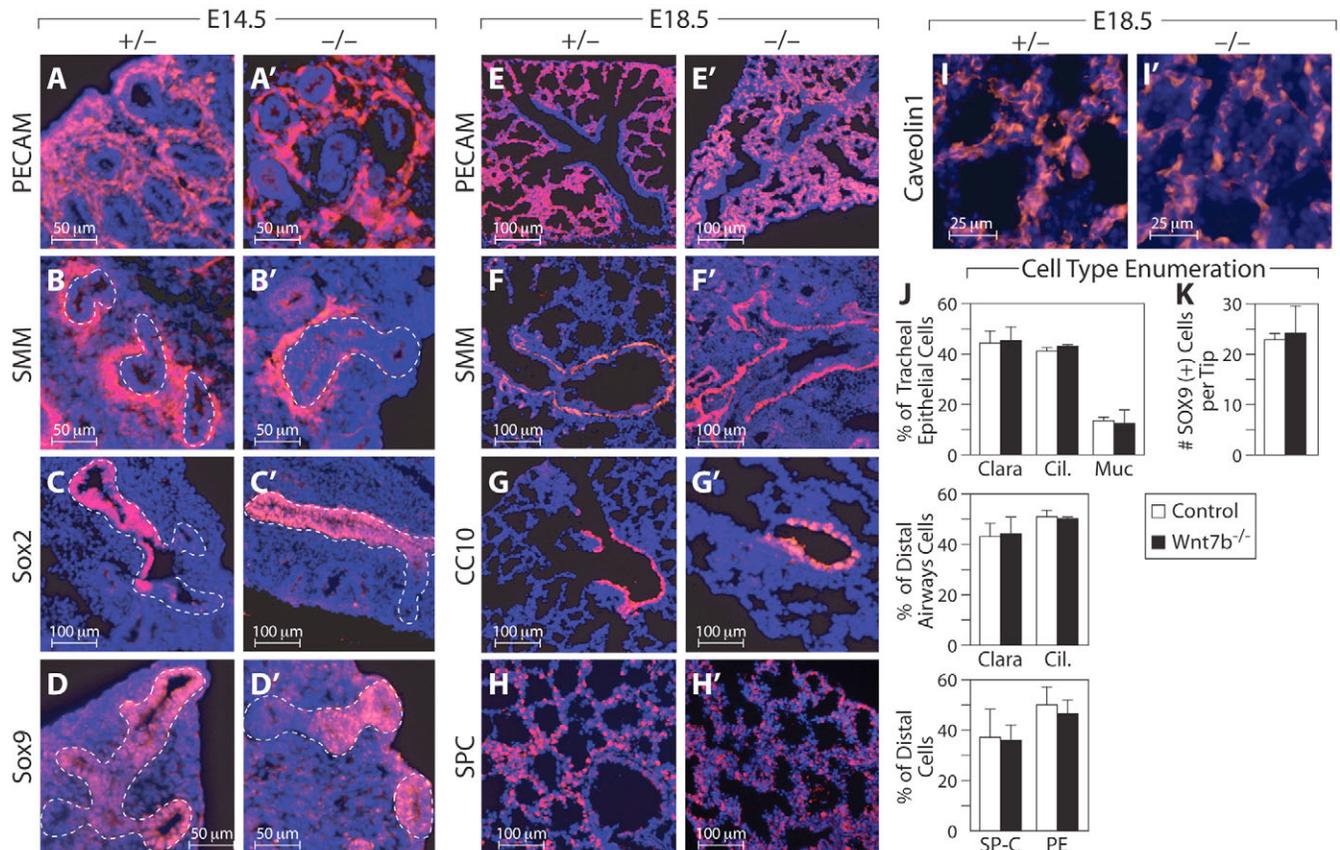
Fig. 2. Cell fate specification, timing of differentiation and tissue architecture are unchanged in *Wnt7b*-null lungs. (A-D′) E14.5 immunohistochemistry of heterozygous (A-D) and *Wnt7b* mutant (A′-D′) mouse lungs. Blood vessels appear normal in the mutant, as marked by PECAM (A,A′), as does airway smooth muscle, marked by smooth muscle myosin (B,B′). Proximal Sox2 (C,C′) and distal Sox9 (D,D′) expression are unchanged in mutants. Dotted lines encircle the epithelium. (**E-I′**) At E18.5, immunohistochemistry of heterozygous (E-I) and *Wnt7b* mutant (E′-I′) lungs demonstrates that blood vessels (E,E′), airway smooth muscle cells (F,F′), Clara cells as marked by CC10 (G,G′), and type 2 cells as marked by surfactant protein C (H,H′) are unchanged in mutant lungs. Type 1 cells marked by caveolin 1 (I,I′) are decreased in number. (**J**) Quantification of cell types in E18.5 lungs demonstrates that the proportions of Clara, ciliated and mucous cells are unchanged in the trachea and airways of *Wnt7b* mutants. In the distal saccules, the proportions of cells positive for SP-C or PECAM are also unchanged. Error bars represent 1 s.d. (**K**) The number of Sox9-positive cells per lung bud tip at E14.5 is unchanged in *Wnt7b* mutants.

At E18.5, Clara cells, ciliated cells, and mucous cells each were present in their usual ratios (Fig. 2J). Mucous cells were appropriately absent in *Wnt7b* mutant bronchi. Even the subtle increase in the relative percentage of ciliated cells to Clara cells that is normally seen in bronchi as compared with trachea (Fig. 2J), occurred normally in mutant lungs (Fig. 2J). At E18.5, SP-C-positive type 2 cells comprised ~37% of the cells in both wild-type and mutant lungs (Fig. 2J). The percentage of PECAM-staining cells was not significantly altered, comprising 49% of total cells in controls and 46% in mutant lungs (Fig. 2J). The filamentous staining of type 1 cells for caveolin 1 precluded rigorous quantitation, but a qualitative reduction in type 1 cell number was seen. Finally, we quantified the number of distal epithelial progenitor cells per tip by counting Sox9-positive cells at E14.5 (Liu and Hogan, 2002; Okubo et al., 2005). We found that the number of Sox9-positive cells per lung bud tip was unchanged, with a mean of 24 cells per tip on cross-section (Fig. 2K). However, as the *Wnt7b* mutant lung contains fewer lung bud tips, the total number of epithelial progenitor cells in the mutant lung is reduced.

We also observed that the timing of differentiation proceeds at its usual pace in mutant lung. Smooth muscle cells, endothelial cells and Sox2-positive epithelial cells were present from E11.5. Sox9-positive cells were present in the distal tip at E11.5, but by E16.5 they were

only present in scattered endoderm tips, as was the case in wild-type lungs. CC10 was first detected at E16.5 of both wild-type and mutant lungs, and SP-C was appropriately restricted to nascent type 2 progenitors at E16.5. We also noted that the general architectural features associated with lung development occurred normally in the *Wnt7b* mutant: smooth muscle surrounded airways proximal to the bronchoalveolar duct junction; the normal boundary between distal Sox9-positive cells and proximal Sox2-positive cells was preserved; and at E16.5 there was a normal thinning of the epithelium and mesenchyme (Fig. 2E-H).

To further characterize the differentiation and patterning in the *Wnt7b* mutant lung, we analyzed the expression of a panel of factors chosen for their distinct expression patterns within the developing lung. A genome-scale ISH screen was performed with E14.5 embryonic mouse lungs using a recently developed transcription factor library that includes ~1100 mouse transcription factors (Gray et al., 2004; Zhou et al., 2007). We identified transcription factors with distinct expression patterns during normal lung organogenesis. The expression of a subset of these genes with stereotyped patterns was compared in *Wnt7b* mutant and wild-type lungs. Their expression in the mutant was found to be normal (see Fig. S5 in the supplementary material). This analysis included genes expressed predominantly in

distal endoderm at E14.5 (*Etv5*, *Spry2*, *Foxa1*, *Foxa2* and *Foxp4*), in proximal endoderm stalks (*Sox2* and *Foxj1*), pulmonary artery (*Epas1*), distal endothelial cells (*Heyl*), cartilaginous rings (*Sox5long*, *Sox9*, *Irx2*) and smooth muscle (*Tgfb1i1*). Genes identified as pan-mesenchymal [*Hoxa2*, *Hoxb5*, *Pod1* (*Tcf21*) and *Osr1*] or periendodermal (*Foxf1*, *Gli2* and *Tbx4*) were also expressed normally in mutant lungs. All these results are consistent with the general finding that *Wnt7b* mutant lungs are small but patterned normally.

Proportionate decrease in the replication of epithelial and mesenchymal progenitors of *Wnt7b*-null lungs

Cells of the distal endoderm tip and the distal mesenchyme proliferate rapidly and are thought to harbor multipotent progenitor cells (Fig. 3A) (Eblaghie et al., 2006; Hogan, 1999; Liu and Hogan, 2002; Okubo et al., 2005). Since some previously described hypoplastic mutant lungs display an increased rate of apoptosis (Eblaghie et al., 2006; Okubo et al., 2005), we performed TUNEL staining to see whether cell death could explain the hypoplasia of *Wnt7b*-null lungs. TUNEL-positive nuclei occurred very rarely in E14.5 mutant and control lung (Fig. 3B,C). No increased apoptosis was noted at E12.5, prior to the dramatic discrepancy in size of mutant lungs (data not shown). We therefore performed BrdU staining to assess whether decreased cell proliferation causes the hypoplasia in *Wnt7b*-null lungs. Replication in the wild-type endoderm was greatest at the distal-most tip of the lung bud (Fig. 3D), whereas in the mesenchyme BrdU labeling was most concentrated in a cap of cells between the endoderm tip and mesothelium (Fig. 3A). BrdU labeling was decreased in both mutant lung endoderm (most prominently at the endoderm tip) and cells of the adjacent mesenchyme throughout development (Fig. 3D,E). In distal tip endoderm, cell labeling decreased from 80% to 50% (Fig. 3F). Similarly, in the adjacent mesenchyme, cell labeling decreased from 90% to 50% (Fig. 3F). Thus, the fraction of BrdU-positive cells decreased by a similar proportion in both the endoderm and the mesenchyme. This contrasts with the finding in the hypomorphic *Wnt7b*[lacZ] homozygotes, in which only mesenchymal proliferation was decreased during a narrow window of time in development (Shu et al., 2002).

Many signaling pathways that modulate cell replication and differentiation are unchanged in *Wnt7b*-null lungs

Hypomorphic *Wnt7b*[lacZ] homozygote lungs displayed no abnormalities of growth factor expression, suggesting that Wnt7b acts independently of other signaling cascades known to regulate lung development (Shu et al., 2002). We revisited growth factor expression in *Wnt7b*-null lungs. Since sonic hedgehog (Shh) exerts a proliferative effect on mesenchyme (Weaver et al., 2003), we examined *Wnt7b*-null lungs for evidence of aberrant hedgehog (Hh) signaling. Expression of *Shh* was confined to the endoderm of the mutant lung in a normal pattern (Fig. 4A and see Fig. S5 in the supplementary material). *Gli1*, a Shh target gene, was also expressed normally in the periendodermal mesenchyme (Fig. 4B and see Fig. S5 in the supplementary material). *Ptch1* and *Hip1* were also expressed normally (Chuang and McMahon, 1999) (Fig. 4C and see Fig. S5 in the supplementary material), as was *Foxf1*, a mesenchymal target of Shh (data not shown). Similarly, *Fgf9*, which is upstream of Shh signaling (White et al., 2006), was properly expressed in the mesothelium and the endoderm tips (see Fig. S5 in the supplementary material). Finally, mesenchymal *Bmp4* expression, which is modulated by Shh signaling (Bitgood and McMahon, 1995; Weaver et al., 2000), was unchanged
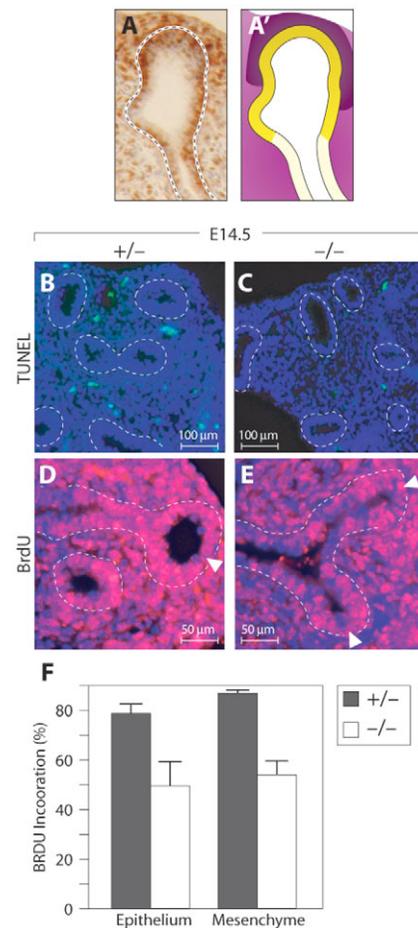

Fig. 3. Deletion of *Wnt7b* results in proportionate decreases in replication of epithelial and mesenchymal tip cells. (A,A') Schematic depiction (A') of BrdU staining (brown) of E14.5 lung bud tip (A). Replication is highest in tip epithelium (A', dark yellow) and tip mesenchyme (A', dark purple) as compared with proximal epithelium (A', light yellow) and mesenchyme (A', light purple). **(B,C)** TUNEL staining of E14.5 wild-type (B) and *Wnt7b* mutant (C) mouse lungs shows no increase in apoptosis in the mutant. Dotted lines encircle epithelium. **(D,E)** BrdU staining of E14.5 wild-type (D) and mutant (E) lungs demonstrates decreased replication in mesenchymal and epithelial cells of the mutant. Arrowheads point to the tips. Dotted lines encircle epithelium. **(F)** A comparison of the percentage of BrdU-labeled cells in wild-type (gray) and mutant (white) tips demonstrates proportionate drops in epithelial and mesenchymal replication (*P*<0.001).

in the *Wnt7b* mutant (Fig. 5F and see Fig. S5 in the supplementary material). We conclude that Shh signaling is not altered in *Wnt7b* mutant lungs. This is consistent with the observed normal distribution of smooth muscle, which is altered in the absence of Hh signaling (Pepicelli et al., 1998). Conversely, studies have demonstrated that *Wnt7b* expression is not altered in lung mutants with diminished Hh signaling (Chuang and McMahon, 1999; Pepicelli et al., 1998). Therefore, we conclude that Wnt7b and Hh signaling are independent pathways to regulate mesenchymal cell proliferation in the embryonic lung (Chuang and McMahon, 1999; Pepicelli et al., 1998).

We next examined the expression of *Fgf10*, an epithelial mitogen and a regulator of branch outgrowth (Bellusci et al., 1997b; Sekine et al., 1999; Weaver et al., 2000). *Wnt7b* mutants demonstrated a modest, variable decrease of *Fgf10* expression in the interbud distal mesenchyme, with preserved proximal mesenchymal expression
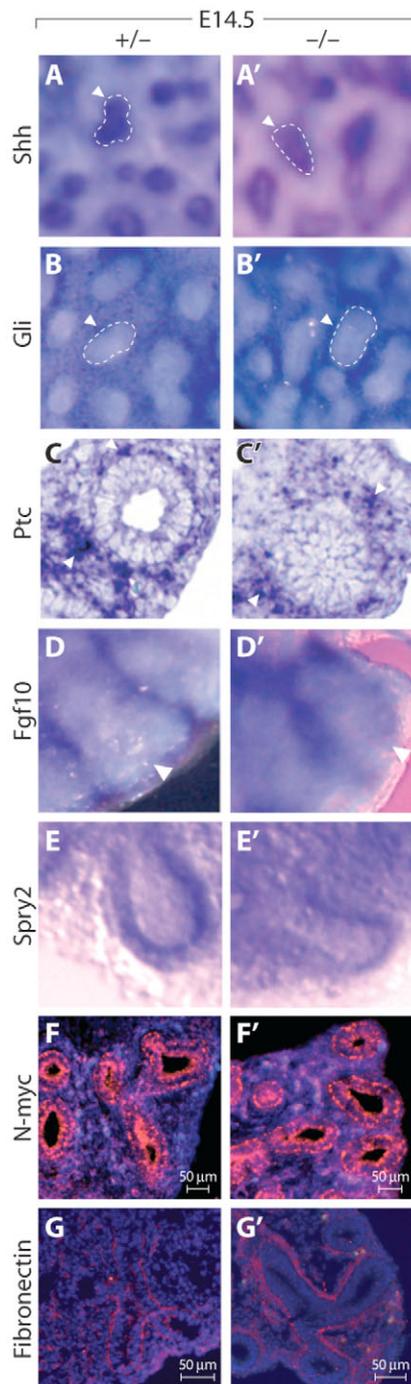
DEVELOPMENT

Fig. 4. Preserved expression of many factors affecting growth in *Wnt7b* mutant lungs. (**A-E'**) E14.5 ISH of *Wnt7b* mutant (A'-E') and control (A-E) mouse lungs. Expression of *Shh* (A,A'), *Gli1* (B,B'), *Ptch1* (C,C') and *Spry2* (E,E') are unchanged in the mutant. The epithelial tip is encircled. *Fgf10* staining (D,D') is largely preserved in mutant lungs; there is a variable decrease in the most-distal expression of *Fgf10* in mutant lungs (arrowhead). (**F-G'**) E14.5 immunohistochemistry for N-myc (F,F') and fibronectin expression (G,G') showing that these are unchanged in the mutant. ISH signal (purple) is indicated by the arrowheads.

(Fig. 4D and see Fig. S5 in the supplementary material). However, the expression of *Spry2*, a known epithelial target and antagonist of mesenchymal Fgf10 signaling (Mailleux et al., 2001), was expressed

normally in the distal tip epithelium (Fig. 4E). The expression of other Wnt genes and *Dkk1* was also unchanged in *Wnt7b* mutant lungs (see Fig. S5 in the supplementary material; data not shown). N-myc (Mycn – Mouse Genome Informatics), which is proposed to be a Wnt target, regulates the proliferation and differentiation of distal lung epithelial progenitors (Okubo et al., 2005). However, N-myc protein expression was normal in mutant lungs (Fig. 4F). Fibronectin, which has also been identified as a downstream target of canonical Wnt signaling (De Langhe et al., 2005), was deposited similarly in mutant and control lungs (Fig. 4G).

Canonical Wnt target genes are absent in the mesenchyme of *Wnt7b*-null lungs

We next examined the expression of Wnt target genes. *Axin2* expression was observed in the endoderm tips of wild-type lungs, consistent with prior reports of epithelial canonical Wnt signaling (Fig. 5A) (De Langhe et al., 2005; Dean et al., 2005; Okubo and Hogan, 2004; Shu et al., 2005). As previously described, *Axin2* and *Lef1* were also expressed in the mesenchyme immediately surrounding the distal endoderm (De Langhe et al., 2005; Jho et al., 2002; Tebar et al., 2001). *Wnt7b*-null lungs did not express either of these genes in mesenchyme or endoderm. This suggests that the canonical Wnt signal being received in the endoderm and the adjacent periendodermal mesenchyme is epithelial Wnt7b.

Epithelial Wnt7b sends a paracrine canonical signal to adjacent mesenchyme cells

To test the hypothesis that mesenchyme responds to a canonical Wnt signal, we employed organ culture. E12.5 embryonic lungs grown at an air-liquid interface exhibited normal *Axin2* and *Lef1* expression (Fig. 5B). Lungs with recombinant Dkk1, which has previously been shown to downregulate canonical Wnt signaling in lung bud culture (De Langhe et al., 2005), displayed reduced *Axin2* and *Lef1* expression. Lungs cultured with lithium to stimulate canonical Wnt signaling showed upregulated *Axin2* and *Lef1* expression through much of the distal mesenchyme (Fig. 5B). The ectopic expression of these Wnt target genes, which are normally restricted to the periendodermal mesenchyme, suggests that the mesenchyme is broadly competent to transduce a canonical Wnt signal.

To further test the hypothesis that the mesenchyme responds to an endodermal signal, we performed tissue recombination. When dissected mesenchyme was cultured in isolation, there was no expression of canonical Wnt target genes (Fig. 5C). When dissected epithelial buds were reaggregated with isolated mesenchyme, the endoderm and mesoderm reassociated and branching morphogenesis resumed. When recombined endoderm-mesenchyme cultures were analyzed, Wnt target gene expression was restored in periendodermal mesenchyme (Fig. 5C), confirming that endoderm is the origin of a canonical Wnt signal.

We next examined *Wnt7b* mutant lungs. As anticipated, these lungs did not express *Axin2* or *Lef1* (Fig. 5D). However, when lithium was added, the expression of these Wnt target genes was restored (Fig. 5D). Thus, Wnt7b signals directly to adjacent competent mesenchyme through a canonical Wnt signaling pathway and is responsible for the periendodermal expression of Wnt target genes in the mesenchyme immediately adjacent to the growing distal tip epithelium. This is consistent with prior reports showing that mesenchymal Fzd1 binds Wnt7b, and that Wnt7b can act through the canonical pathway (Wang et al., 2005). Since the mesenchyme seems broadly competent to receive a canonical Wnt signal, we suggest that the short range of action of Wnt7b creates a zone of induction in the periendodermal cells, which correspond to the most
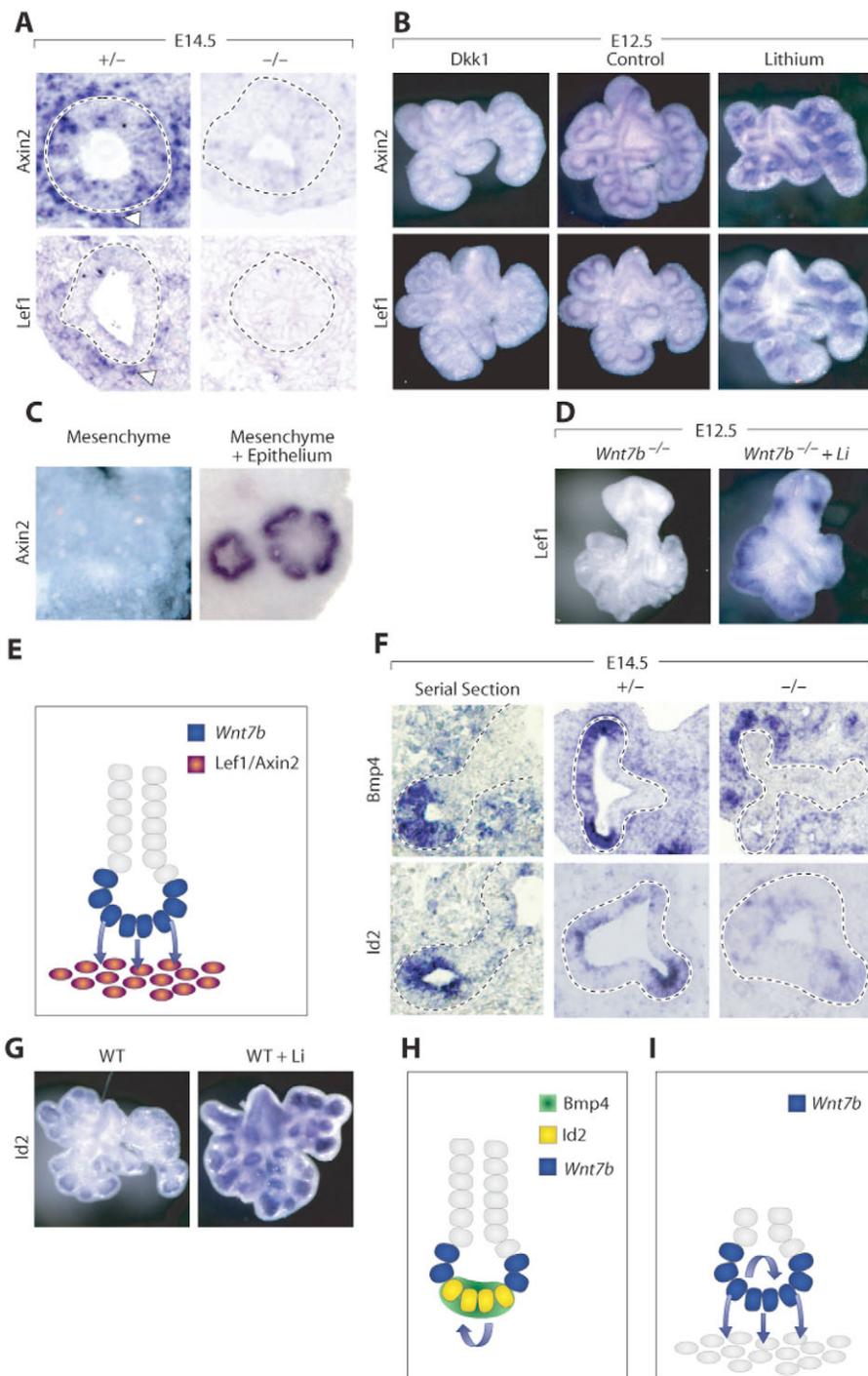
Fig. 5. Mechanism of Wnt7b action in mouse lung development. (**A**) ISH showing loss of canonical Wnt targets in mesenchyme and endoderm of *Wnt7b* mutant lungs. Dotted lines encircle epithelium. Arrowheads point to periendodermal mesenchyme. (**B**) E12.5 whole-mount ISH of *Axin2* and *Lef1* in cultured wild-type lungs. Wnt signaling is decreased with the addition of Dkk1 (left) and enhanced by lithium (right) when compared with control cultures (middle). In lithium-treated lungs, mesenchymal staining of the canonical targets has expanded. (**C**) *Axin2* expression in mesenchyme cultured alone and in mesenchyme recombined with epithelium, showing that mesenchymal *Axin2* expression requires endoderm induction. (**D**) Lithium rescues *Lef1* expression in E12.5 mutant lungs when compared with *Wnt7b* mutant lungs cultured without lithium. (**E**) Epithelial Wnt7b activates a canonical pathway in neighboring mesenchyme. (**F**) *Bmp4* and *Id2* expression are coincident on serial sections of E14.5 wild-type lung (left). Expression of epithelial *Bmp4* and *Id2* are decreased in mutant lungs (middle and right). (**G**) Lithium induces ectopic *Id2* expression in cultured E12.5 wild-type lungs. (**H**) Wnt7b induces Bmp4 and Id2 production in endoderm tip cells. (**I**) Wnt7b coordinately activates autocrine and paracrine signaling cascades to increase cell replication.

actively dividing mesenchymal progenitors (Fig. 3A, Fig. 5E). Coupled with the normal expression of the mesenchymal mitogens Shh and Fgf9, this is consistent with a direct mitogenic effect of Wnt7b on the lung mesenchyme.

Removal of Wnt7b results in decreased epithelial Bmp signaling and *Id2* expression

When we screened *Wnt7b* mutant lungs for altered epithelial transcription factor expression, we identified decreased distal tip *Id2* expression (Fig. 5F and see Fig. S5 in the supplementary material). Other molecules expressed in the tip epithelium, including Etv5,

Sox9 and N-myc, were expressed normally in the *Wnt7b* mutant. Since the localizations of epithelial *Bmp4* and *Id2* are coincident (Fig. 5F), we examined the epithelial expression of *Bmp4* and noted that it is reduced in *Wnt7b* mutants (Fig. 5F and see Fig. S5 in the supplementary material). By contrast, mesenchymal *Bmp4* expression, regulated by Shh (Weaver et al., 2003), remained normal (Fig. 5F).

Canonical Wnt signaling has previously been demonstrated to be upstream of epithelial *Bmp4* expression (Shu et al., 2005). We sought to confirm the hypothesis that *Id2* is also an endodermal Wnt target. Cultured wild-type lungs expressed *Id2* only in the most distal

epithelium (Fig. 5G). However, when lithium was added, *Id2* expression at the distal tip was upregulated (Fig. 5G). In addition, ectopic production of *Id2* occurred in proximal endoderm (Fig. 5G). Interestingly, addition of Bmp4 protein to the culture medium does not lead to an increase in *Id2* expression, although Bmp4 does produce characteristic changes in bud morphology (data not shown). This suggests that *Id2* expression is not downstream of Bmp4 signaling. The decrease in *Id2* and *Bmp4* expression in *Wnt7b* mutant lungs identifies Wnt7b as the source of an autocrine canonical signal (Fig. 5H). Bmp4 has been shown to act as an autocrine regulator of distal endoderm progenitor cell replication (Eblaghie et al., 2006). Thus, the decrease in *Bmp4* expression explains, at least in part, the decreased rate of epithelial proliferation observed in *Wnt7b*-null lungs.

DISCUSSION
Analysis of the null *Wnt7b*^{D3} allele reveals previously unappreciated functions of Wnt7b in lung development

We show that a prior model of *Wnt7b* deletion, using the *Wnt7b*^{D1} allele (Lobov et al., 2005), is hypomorphic due to the presence of an alternative exon 1. Based on the presence of *Wnt7b*-exon-3-containing mRNA transcripts in the *Wnt7b*^{lacZ} model, this allele is likely to display alternative exon 1 splicing, as would be predicted on the basis of its genomic sequence. We further note that the *Wnt7b*^{lacZ} allele retains a constitutive promoter and neomycin resistance cassette that is not present in the *Wnt7b*^{D3} allele. In fact, the presence of this cassette in a prior version of the *Wnt7b*^{D1} allele caused early E9.5 embryonic lethality (distinct from and earlier than the placental abnormalities found in *Wnt7b*-null mice with cardiovascular and anteroposterior patterning abnormalities; data not shown). This neomorphic phenotype was completely eliminated by removing the constitutive promoter and neomycin cassette. In addition, we identified the presence of an unannotated cDNA (Unigene accession #Mm.394884), the 5′ sequence of which overlaps in opposite orientation with *Wnt7b* exon 1. An alteration of this gene product or a neomorphic effect of the neomycin resistance cassette could account for elements of the phenotype of *Wnt7b*^{lacZ} animals, most notably the vascular smooth muscle abnormalities that are not seen in true null *Wnt7b*^{D3} animals (Shu et al., 2002).

Analysis of the lungs of *Wnt7b*^{D3} homozygotes reveals a number of new findings, including a reduction in the replication of both epithelium and mesenchyme, in contrast to the previously reported reduction in mesenchyme proliferation (Shu et al., 2002). Additionally, we demonstrate defects in tracheal cartilage formation and minor branching abnormalities not seen in *Wnt7b*^{lacZ} homozygotes. Most importantly, a characterization of the lung hypoplasia in these true null mice demonstrates that Wnt7b interacts with known signaling cascades in the lung and activates a canonical signaling cascade in both mesenchyme and epithelium. The analysis of the hypomorphic *Wnt7b*^{lacZ} animals, by contrast, demonstrated no such interactions, implying that Wnt7b was independent of these signaling pathways.

Importantly, we see no abnormalities in smooth muscle development or apoptosis as previously noted in *Wnt7b*^{lacZ} animals (Shu et al., 2002). The greater large vessel hemorrhage seen in these animals was likely to have been potentiated by smooth muscle irregularity and apoptosis. In *Wnt7b*^{D3} true null animals, small vessel and large vessel hemorrhage occur with equal frequency, and are likely to be a consequence of the pulmonary hypertension that results from vascular hypoplasia in the setting of normal cardiac size.

A decrease in replication of epithelium and mesenchyme in *Wnt7b* mutants results in a small lung with preserved differentiation and architecture

Wnt signaling in the lung has been proposed to modulate the behavior of distal progenitor cells (Cardoso and Lu, 2006; Perl et al., 2002; Warburton et al., 2000). Wnts have been proposed to stimulate the replication of tip progenitors, to inhibit the differentiation of tip progenitors, and to modulate tip progenitors to alter the ratio of proximal to distal cell differentiation (Cardoso and Lu, 2006; De Langhe et al., 2005; Liu and Hogan, 2002; Mucenski et al., 2003; Okubo and Hogan, 2004; Okubo et al., 2005; Weaver et al., 2000). The hypoplastic phenotype of *Wnt7b*^{D3} homozygous animals is caused by a similar decrease in proliferation of both epithelium and mesenchyme, resulting in the diminished production of differentiated cells, which, nonetheless, largely retain their normal patterning and tissue geometry. Interestingly, the number of Sox9-positive epithelial progenitors within a given lung bud tip does not change. Surprisingly, the time-course of differentiation proceeds normally despite this decrease in cell division. This suggests that the mechanisms regulating the timing of cell differentiation can be partly uncoupled from the mechanisms that regulate cell replication.

Epithelial Wnt7b activates an autocrine and a paracrine canonical signaling cascade in adjacent pools of endoderm and mesenchyme

Wnt7b induces a canonical Wnt signaling cascade in adjacent epithelium and mesenchyme. Previous studies using Wnt-reporter lines did not demonstrate canonical Wnt reception within the mesenchyme (De Langhe et al., 2005; Dean et al., 2005; Okubo and Hogan, 2004; Shu et al., 2005). However, the mesenchymal expression of the Wnt target genes *Axin2* and *Lef1* (Jho et al., 2002; Tebar et al., 2001), and mesenchymal β-catenin staining (Shu et al., 2005; Tebar et al., 2001), have been previously noted. We now show that lung mesenchyme is broadly competent to transduce a canonical Wnt signal, and suggest that the periendodermal restriction of canonical Wnt activity is due to a local action of Wnt7b (Lobov et al., 2005). As Wnt-reporter mice do not capture the entire array of Wnt signaling events (Dean et al., 2005; He et al., 2004), it will be of interest to re-examine reports of altered Wnt signaling in the lung in light of this new finding.

Wnt7b also activates a canonical signaling cascade in the endoderm to induce the expression of *Bmp4* and *Id2*. Our findings are consistent with prior work that establishes that Wnt signaling is upstream of Bmp4 (Shu et al., 2005) and that Wnt7b is able to transduce a canonical Wnt signal in vitro (Wang et al., 2005). Bmp4 signaling regulates the proliferation of distal tip epithelial cells (Eblaghie et al., 2006), and we suggest that Wnt7b, at least in part, stimulates the autocrine amplification of progenitor cell replication through this mechanism. Id2 is also known to stimulate cell proliferation in many contexts (Kowanetz et al., 2004; Lasorella et al., 2002; Memezawa et al., 2007; Nigten et al., 2005; Yokota et al., 2001) and is located downstream of Bmp4 in other systems (Hollnagel et al., 1999; Hua et al., 2006; Ying et al., 2003). Our preliminary in vitro experiments suggest, however, that in lung epithelium, *Bmp4* and *Id2* might be parallel rather than serial targets of Wnt signaling. Further experiments will be necessary to clarify the epistatic relationships of *Id2* and *Bmp4* as well as the precise function of Id2, as *Id2*-null mice do not display an overt pulmonary phenotype (Yokota et al., 1999; Yokota et al., 2000). Efforts to phenotypically rescue *Wnt7b*-null lungs in culture with Fgf10 protein, Bmp4 protein, and Wnt7b-expressing cell lines were

difficult to interpret owing to variable rates and patterns of BrdU incorporation in embryonic lungs grown in vitro. In summary, we propose that Wnt7b produced in the distal lung bud epithelium induces signaling cascades in both tip epithelial progenitors and adjacent mesenchyme (Fig. 5I). We hypothesize that the previously described short range of action of Wnt7b (Lobov et al., 2005) causes it, at least in part, to delimit the populations of greatest replicative activity in the embryonic lung to adjacent pools of cells located in the distal lung bud tip.

Wnt7b and lung size

The loss of Wnt7b results in the decreased replication of both epithelium and mesenchyme without grossly perturbing cell differentiation or lung architecture. This surprisingly specific result contrasts with the hypoplastic phenotypes associated with the deletion of many mitogenic factors, such as Shh, which also act to modify cell fate. Given the Wnt7b phenotype, it is therefore not surprising that Hh signaling is unchanged in *Wnt7b*-null lungs. Similarly, in the epithelium, *Wnt7b* expression results in a highly localized increase of only epithelial *Bmp4* expression. More profound alterations in either Bmp or Wnt signaling might be predicted to cause changes in cell fate, based on prior observations (Okubo and Hogan, 2004; Weaver et al., 2000; Weaver et al., 1999). We speculate that such subtle modulation of mitogenic activity might be a characteristic of molecules that result in changes in growth without large effects on differentiation.

The *Fgf9*-null mouse is the only other mutant animal to display such profound growth defects in the absence of significant patterning abnormalities (Colvin et al., 2001). Although Fgf9 may have a disproportionate effect on mesenchyme proliferation (Colvin et al., 2001), reports do suggest that Fgf9 can also stimulate epithelial proliferation and alter smooth muscle and vascular development (del Moral et al., 2006; White et al., 2007; White et al., 2006). *Fgf9* expression, however, remains normal in *Wnt7b*-null mice (see Fig. S5 in the supplementary material; data not shown). Furthermore, *Wnt7b*-null mice display entirely normal Hh signaling, and this pathway is modulated by Fgf9 and is responsible for many of its mitogenic actions on the mesenchyme (White et al., 2006). Interestingly, both *Wnt7b*- and *Fgf9*-null mutants display decreased *Fgf10* expression in the distal interbud region, with preservation of more proximal *Fgf10* expression (Fig. 4D and see Fig. S5 in the supplementary material) (White et al., 2006). Future experiments should examine the interaction of Wnt7b and Fgf9 and their precise relationships to the Bmp4, Shh and Fgf10 cascades. Indeed, the regulation of Wnt antagonists such as Dkk1 can be induced by Fgf9, and may play a role in limiting lung size by antagonizing Wnt7b (De Langhe et al., 2005; del Moral et al., 2006). Similarly, Wnt5a, a non-canonical Wnt, may antagonize Wnt7b function to limit lung growth (De Langhe et al., 2005; Li et al., 2002).

Finally, it is unclear whether lung growth is proportional to Wnt7b dose, or whether there is a threshold level beneath which lung size drops precipitously. Preliminary observations on a set of allelic crosses conducted on an identical genetic background show that mice that possess one $Wnt7b^{D1}$ and one $Wnt7b^{D3-4}$ allele possess an intermediate phenotype, with incomplete tracheal cartilaginous rings but normally sized lungs. This suggests the possibility that the tracheal phenotype is more sensitive to loss of Wnt7b exon 1a than is the lung size phenotype. Unfortunately, we find no combination of alleles that results in graded changes in lung growth. The current lack of understanding of the distinct roles and expression patterns of the two alternatively spliced Wnt7b isoforms clouds interpretation. It is unlikely that the $Wnt7b^{lacZ}$ allele will contribute meaningfully to an allelic series of mutants as $Wnt7b^{lacZ}$ undergoes not only alternative splicing, but also displays a neomorphic phenotype. However, a complete analysis of the remaining combination of alleles on a common background should help clarify the roles of different splice forms of Wnt7b. Since Wnt7b protein has evaded purification, we propose that a genetic model permitting finely regulable, graded Wnt7b expression on a $Wnt7b^{D3}$-null background would permit an analysis of the exact effect of Wnt7b on lung size.

Supplementary material
Supplementary material for this article is available at
http://dev.biologists.org/cgi/content/full/135/9/1625/DC1

References
Bellusci, S., Furuta, Y., Rush, M. G., Henderson, R., Winnier, G. and Hogan, B. L. (1997a). Involvement of Sonic hedgehog (Shh) in mouse embryonic lung growth and morphogenesis. *Development* **124**, 53-63.
Bellusci, S., Grindley, J., Emoto, H., Itoh, N. and Hogan, B. L. (1997b). Fibroblast growth factor 10 (FGF10) and branching morphogenesis in the embryonic mouse lung. *Development* **124**, 4867-4878.
Bitgood, M. J. and McMahon, A. P. (1995). Hedgehog and Bmp genes are coexpressed at many diverse sites of cell-cell interaction in the mouse embryo. *Dev. Biol.* **172**, 126-138.
Cardoso, W. V. and Lu, J. (2006). Regulation of early lung morphogenesis: questions, facts and controversies. *Development* **133**, 1611-1624.
Chuang, P. T. and McMahon, A. P. (1999). Vertebrate Hedgehog signalling modulated by induction of a Hedgehog-binding protein. *Nature* **397**, 617-621.
Colvin, J. S., White, A. C., Pratt, S. J. and Ornitz, D. M. (2001). Lung hypoplasia and neonatal death in Fgf9-null mice identify this gene as an essential regulator of lung mesenchyme. *Development* **128**, 2095-2106.
De Langhe, S. P., Sala, F. G., Del Moral, P. M., Fairbanks, T. J., Yamada, K. M., Warburton, D., Burns, R. C. and Bellusci, S. (2005). Dickkopf-1 (DKK1) reveals that fibronectin is a major target of Wnt signaling in branching morphogenesis of the mouse embryonic lung. *Dev. Biol.* **277**, 316-331.
Dean, C. H., Miller, L. A., Smith, A. N., Dufort, D., Lang, R. A. and Niswander, L. A. (2005). Canonical Wnt signaling negatively regulates branching morphogenesis of the lung and lacrimal gland. *Dev. Biol.* **286**, 270-286.
del Moral, P. M., De Langhe, S. P., Sala, F. G., Veltmaat, J. M., Tefft, D., Wang, K., Warburton, D. and Bellusci, S. (2006). Differential role of FGF9 on epithelium and mesenchyme in mouse embryonic lung. *Dev. Biol.* **293**, 77-89.
Eblaghie, M. C., Reedy, M., Oliver, T., Mishina, Y. and Hogan, B. L. (2006). Evidence that autocrine signaling through Bmpr1a regulates the proliferation, survival and morphogenetic behavior of distal lung epithelial cells. *Dev. Biol.* **291**, 67-82.
Gray, P. A., Fu, H., Luo, P., Zhao, Q., Yu, J., Ferrari, A., Tenzen, T., Yuk, D. I., Tsung, E. F., Cai, Z. et al. (2004). Mouse brain organization revealed through direct genome-scale TF expression analysis. *Science* **306**, 2255-2257.
Hayashi, S., Lewis, P., Pevny, L. and McMahon, A. P. (2002). Efficient gene modulation in mouse epiblast using a Sox2Cre transgenic mouse strain. *Mech. Dev.* **119 Suppl. 1**, S97-S101.
He, X. C., Zhang, J., Tong, W. G., Tawfik, O., Ross, J., Scoville, D. H., Tian, Q., Zeng, X., He, X., Wiedemann, L. M. et al. (2004). BMP signaling inhibits intestinal stem cell self-renewal through suppression of Wnt-beta-catenin signaling. *Nat. Genet.* **36**, 1117-1121.
Hogan, B. L. (1999). Morphogenesis. *Cell* **96**, 225-233.
Hollnagel, A., Oehlmann, V., Heymer, J., Ruther, U. and Nordheim, A. (1999). Id genes are direct targets of bone morphogenetic protein induction in embryonic stem cells. *J. Biol. Chem.* **274**, 19838-19845.
Hua, H., Zhang, Y. Q., Dabernat, S., Kritzik, M., Dietz, D., Sterling, L. and Sarvetnick, N. (2006). BMP4 regulates pancreatic progenitor cell expansion through Id2. *J. Biol. Chem.* **281**, 13574-13580.
Jho, E. H., Zhang, T., Domon, C., Joo, C. K., Freund, J. N. and Costantini, F. (2002). Wnt/beta-catenin/Tcf signaling induces the transcription of Axin2, a negative regulator of the signaling pathway. *Mol. Cell. Biol.* **22**, 1172-1183.
Kowanetz, M., Valcourt, U., Bergstrom, R., Heldin, C. H. and Moustakas, A. (2004). Id2 and Id3 define the potency of cell proliferation and differentiation responses to transforming growth factor beta and bone morphogenetic protein. *Mol. Cell. Biol.* **24**, 4241-4254.

Lasorella, A., Boldrini, R., Dominici, C., Donfrancesco, A., Yokota, Y., Inserra, A. and Iavarone, A. (2002). Id2 is critical for cellular proliferation and is the oncogenic effector of N-myc in human neuroblastoma. *Cancer Res.* **62**, 301-306.

Li, C., Xiao, J., Hormi, K., Borok, Z. and Minoo, P. (2002). Wnt5a participates in distal lung morphogenesis. *Dev. Biol.* **248**, 68-81.

Liu, Y. and Hogan, B. L. (2002). Differential gene expression in the distal tip endoderm of the embryonic mouse lung. *Gene Expr. Patterns* **2**, 229-233.

Lobov, I. B., Rao, S., Carroll, T. J., Vallance, J. E., Ito, M., Ondr, J. K., Kurup, S., Glass, D. A., Patel, M. S., Shu, W. et al. (2005). WNT7b mediates macrophage-induced programmed cell death in patterning of the vasculature. *Nature* **437**, 417-421.

Mailleux, A. A., Tefft, D., Ndiaye, D., Itoh, N., Thiery, J. P., Warburton, D. and Bellusci, S. (2001). Evidence that SPROUTY2 functions as an inhibitor of mouse embryonic lung growth and morphogenesis. *Mech. Dev.* **102**, 81-94.

Memezawa, A., Takada, I., Takeyama, K., Igarashi, M., Ito, S., Aiba, S., Kato, S. and Kouzmenko, A. P. (2007). Id2 gene-targeted crosstalk between Wnt and retinoid signaling regulates proliferation in human keratinocytes. *Oncogene* **26**, 5038-5045.

Mucenski, M. L., Wert, S. E., Nation, J. M., Loudy, D. E., Huelsken, J., Birchmeier, W., Morrisey, E. E. and Whitsett, J. A. (2003). beta-Catenin is required for specification of proximal/distal cell fate during lung morphogenesis. *J. Biol. Chem.* **278**, 40231-40238.

Nigten, J., Breems-de Ridder, M. C., Erpelinck-Verschueren, C. A., Nikoloski, G., van der Reijden, B. A., van Wageningen, S., van Hennik, P. B., de Witte, T., Lowenberg, B. and Jansen, J. H. (2005). ID1 and ID2 are retinoic acid responsive genes and induce a G0/G1 accumulation in acute promyelocytic leukemia cells. *Leukemia* **19**, 799-805.

Okubo, T. and Hogan, B. L. (2004). Hyperactive Wnt signaling changes the developmental potential of embryonic lung endoderm. *J. Biol.* **3**, 11.

Okubo, T., Knoepfler, P. S., Eisenman, R. N. and Hogan, B. L. (2005). Nmyc plays an essential role during lung development as a dosage-sensitive regulator of progenitor cell proliferation and differentiation. *Development* **132**, 1363-1374.

Parr, B. A., Cornish, V. A., Cybulsky, M. I. and McMahon, A. P. (2001). Wnt7b regulates placental development in mice. *Dev. Biol.* **237**, 324-332.

Pepicelli, C. V., Lewis, P. M. and McMahon, A. P. (1998). Sonic hedgehog regulates branching morphogenesis in the mammalian lung. *Curr. Biol.* **8**, 1083-1086.

Perl, A. K., Wert, S. E., Nagy, A., Lobe, C. G. and Whitsett, J. A. (2002). Early restriction of peripheral and proximal cell lineages during formation of the lung. *Proc. Natl. Acad. Sci. USA* **99**, 10482-10487.

Rawlins, E. L. and Hogan, B. L. (2006). Epithelial stem cells of the lung: privileged few or opportunities for many? *Development* **133**, 2455-2465.

Sekine, K., Ohuchi, H., Fujiwara, M., Yamasaki, M., Yoshizawa, T., Sato, T., Yagishita, N., Matsui, D., Koga, Y., Itoh, N. et al. (1999). Fgf10 is essential for limb and lung formation. *Nat. Genet.* **21**, 138-141.

Shu, W., Jiang, Y. Q., Lu, M. M. and Morrisey, E. E. (2002). Wnt7b regulates mesenchymal proliferation and vascular development in the lung. *Development* **129**, 4831-4842.

Shu, W., Guttentag, S., Wang, Z., Andl, T., Ballard, P., Lu, M. M., Piccolo, S., Birchmeier, W., Whitsett, J. A., Millar, S. E. et al. (2005). Wnt/beta-catenin signaling acts upstream of N-myc, BMP4, and FGF signaling to regulate proximal-distal patterning in the lung. *Dev. Biol.* **283**, 226-239.

Tebar, M., Destree, O., de Vree, W. J. and Ten Have-Opbroek, A. A. (2001). Expression of Tcf/Lef and sFrp and localization of beta-catenin in the developing mouse lung. *Mech. Dev.* **109**, 437-440.

Wang, Z., Shu, W., Lu, M. M. and Morrisey, E. E. (2005). Wnt7b activates canonical signaling in epithelial and vascular smooth muscle cells through interactions with Fzd1, Fzd10, and LRP5. *Mol. Cell. Biol.* **25**, 5022-5030.

Warburton, D., Schwarz, M., Tefft, D., Flores-Delgado, G., Anderson, K. D. and Cardoso, W. V. (2000). The molecular basis of lung morphogenesis. *Mech. Dev.* **92**, 55-81.

Weaver, M., Yingling, J. M., Dunn, N. R., Bellusci, S. and Hogan, B. L. (1999). Bmp signaling regulates proximal-distal differentiation of endoderm in mouse lung development. *Development* **126**, 4005-4015.

Weaver, M., Dunn, N. R. and Hogan, B. L. (2000). Bmp4 and Fgf10 play opposing roles during lung bud morphogenesis. *Development* **127**, 2695-2704.

Weaver, M., Batts, L. and Hogan, B. L. (2003). Tissue interactions pattern the mesenchyme of the embryonic mouse lung. *Dev. Biol.* **258**, 169-184.

Weidenfeld, J., Shu, W., Zhang, L., Millar, S. E. and Morrisey, E. E. (2002). The WNT7b promoter is regulated by TTF-1, GATA6, and Foxa2 in lung epithelium. *J. Biol. Chem.* **277**, 21061-21070.

White, A. C., Xu, J., Yin, Y., Smith, C., Schmid, G. and Ornitz, D. M. (2006). FGF9 and SHH signaling coordinate lung growth and development through regulation of distinct mesenchymal domains. *Development* **133**, 1507-1517.

White, A. C., Lavine, K. J. and Ornitz, D. M. (2007). FGF9 and SHH regulate mesenchymal Vegfa expression and development of the pulmonary capillary network. *Development* **134**, 3743-3752.

Ying, Q. L., Nichols, J., Chambers, I. and Smith, A. (2003). BMP induction of Id proteins suppresses differentiation and sustains embryonic stem cell self-renewal in collaboration with STAT3. *Cell* **115**, 281-292.

Yokota, Y., Mansouri, A., Mori, S., Sugawara, S., Adachi, S., Nishikawa, S. and Gruss, P. (1999). Development of peripheral lymphoid organs and natural killer cells depends on the helix-loop-helix inhibitor Id2. *Nature* **397**, 702-706.

Yokota, Y., Mori, S., Nishikawa, S. I., Mansouri, A., Gruss, P., Kusunoki, T., Katakai, T. and Shimizu, A. (2000). The helix-loop-helix inhibitor Id2 and cell differentiation control. *Curr. Top. Microbiol. Immunol.* **251**, 35-41.

Yokota, Y., Mori, S., Narumi, O. and Kitajima, K. (2001). In vivo function of a differentiation inhibitor, Id2. *IUBMB Life* **51**, 207-214.

Zhou, Q., Law, A. C., Rajagopal, J., Anderson, W. J., Gray, P. A. and Melton, D. A. (2007). A multipotent progenitor domain guides pancreatic organogenesis. *Dev. Cell* **13**, 103-114.